Raman heterodyne interference: Symmetry analysis

E. S. Kintzer, M. Mitsunaga, and R. G. Brewer
IBM Research Laboratory, San Jose, California 95193
and Department of Applied Physics, Stanford University, Stanford, California 94305
(Received 21 December 1984)

The Raman heterodyne interference phenomenon observed recently in the impurity-ion crystals Pr^{3+}:$YAlO_3$ and Pr^{3+}:LaF_3 is examined from the viewpoint of symmetry analysis of the nonlinear susceptibility tensor. General Raman heterodyne signals are derived for all crystal symmetries and for all optical-frequency and radiofrequency polarizations. An example of the utility of this approach resolves a controversy over the crystal symmetry of LaF_3, establishing that it is trigonal rather than hexagonal.

I. INTRODUCTION

Novel interference phenomena[1,2] have been observed in impurity-ion solids using Raman heterodyne detection.[3] The interference is a consequence of the linear dependence of the signal on the participating matrix elements which permits the detection of relative phases as well as amplitudes. Calculations presented in the preceding paper[2] show how the interference can occur between two or more inequivalent nuclear sites or between different Zeeman components of a single site. The drawback of these calculations is that they require a detailed knowledge of the impurity-ion wave functions. In this paper, a group-theoretical approach allows us to analyze Raman heterodyne interference between sites using symmetry arguments. All that is required is a knowledge of the symmetry of the point group for the crystal host and for the nuclear sites. This approach was first introduced by Taylor[4] and will be extended here to include a more general derivation and results for all crystal symmetries. Examples of crystal symmetry arguments and assignments are given for two impurity-ion crystals, Pr^{3+}:$YAlO_3$ and Pr^{3+}:LaF_3, and compared with experiment. The controversy whether LaF_3 has hexagonal or trigonal symmetry is resolved by symmetry analysis and a simple optical polarization experiment reported here.

The symmetry argument that we use is based on Neumann's principle which states that the symmetry of any macroscopic observable of a crystal must be the same as the symmetry of the point group of the crystal. The group-theoretical treatment proceeds as follows. The induced polarization of the optically excited impurity ion in a Raman heterodyne experiment is given by

$$P_i=\chi_{ijk}E_jH_k \quad (i,j,k=x,y,z) , \tag{1}$$

where there is an implied sum over repeated indices. Since the optical field E and the polarization P are polar vectors and the magnetic radiofrequency field H is an axial vector, the nonlinear susceptibility χ is a third-rank axial tensor. The macroscopic χ must be invariant under the symmetry operations of the point group of the host crystal. These operations can lead to a great simplification in the expression for P since some of the 3^3 components of χ will be zero while the remaining nonzero components are not necessarily independent. The symmetry properties of χ are tabulated by Birss.[5]

The macroscopic induced polarization is detected as a heterodyne beat signal S,

$$S=\mathbf{P}\cdot\mathbf{E}=\chi_{ijk}E_iE_jH_k . \tag{2}$$

In principle, this macroscopic signal can be decomposed into the contributions of the individual impurity-ion sites. To examine the sites alone we follow the same procedure as for the macroscopic signal but now we must use the symmetry properties of the point group of the site. Following the notation of Taylor,[4] we denote $\chi^{(m)}$ as the susceptibility of the mth site. Starting with the induced polarization of one site, the polarizations of the remaining sites can be generated using the symmetry operations of the host-crystal point group. Thus, if there are n sites, then there are n-generating matrices $\sigma^{(m)}$ (including the identity). The generator $\sigma^{(m)}$ is used to evaluate $\chi^{(m)}$ according to [5]

$$\chi^{(m)}_{ijk}=\sigma^{(m)}_{ip}\sigma^{(m)}_{jq}\sigma^{(m)}_{kr}\chi^{(1)}_{pqr}(\det\sigma^{(m)}) . \tag{3}$$

The total signal

$$S=\sum_{m=1}^{n}\chi^{(m)}_{ijk}E_iE_jH_k \tag{4}$$

must then equal the macroscopic result (2).

II. SITE INTERFERENCE IN Pr^{3+}:$YAlO_3$

To illustrate this type of calculation, first consider the case of Pr^{3+}:$YAlO_3$ where the host crystal has D_{2h} symmetry[6] (orthorhombic) and the impurity ion Pr^{3+} undergoes the optical transition ${}^3H_4(\Gamma_1)\rightarrow{}^1D_2(\Gamma_1)$ between the lowest crystal-field components of symmetry Γ_1. We choose a space-fixed coordinate system (x,y,z) parallel to the crystal (a,b,c) axes. For this symmetry the only nonvanishing components of χ are xyz, xzy, zxy, yxz, yzx, and zyx (see Table 2e, entry D_3 of Birss[5]). Then the induced macroscopic polarization for general fields $\mathbf{E}=(E_x,E_y,E_z)$ and $\mathbf{H}=(H_x,H_y,H_z)$ is

$$P_x=\chi_{xyz}E_yH_z+\chi_{xzy}E_zH_y ,$$
$$P_y=\chi_{yxz}E_xH_z+\chi_{yzx}E_zH_x ,$$
$$P_z=\chi_{zxy}E_xH_y+\chi_{zyx}E_yH_x .$$

This can be simplified further by restricting the electric field polarization to x and y directions for the electric dipole transition to be allowed between states of Γ_1 symmetry.[7,8] Then $\chi_{xzy}=\chi_{yzx}=\chi_{zxy}=\chi_{zyx}=0$. The detected signal is

$$S=(\chi_{xyz}+\chi_{yxz})E_xE_yH_z . \tag{5}$$

For the site interference experiments reported in Refs. 1 and 2, where $\mathbf{E}=(E_x,E_y,0)$ and $\mathbf{H}=(0,0,H_z)$, the macroscopic signal in zero static magnetic field was observed to be zero within the limit of sensitivity of the experiment, allowing us to conclude in (5) that $\chi_{xyz}+\chi_{yxz}\sim 0$.

We now examine the contribution of the individual Pr^{3+} sites to the macroscopic signal. The site symmetry[6] of Pr^{3+}:$YAlO_3$ is C_{1h}. There are four sites with half of the sites being inversion images of the other half. For C_{1h} the nonzero components of χ are the same as for D_{2h} with the addition of zzz, xxz, and yyz (Table 2e, entry B_3 of Birss[5]). For site 1 the polarization is

$$P_x^{(1)}=\chi_{xyz}^{(1)}E_yH_z+\chi_{xzy}^{(1)}E_zH_y+\chi_{xxz}^{(1)}E_xH_z ,$$
$$P_y^{(1)}=\chi_{yxz}^{(1)}E_xH_z+\chi_{yzx}^{(1)}E_zH_x+\chi_{yyz}^{(1)}E_yH_z , \tag{6}$$
$$P_z^{(1)}=\chi_{zxy}^{(1)}E_xH_y+\chi_{zyx}^{(1)}E_yH_x+\chi_{zzz}^{(1)}E_zH_z .$$

We can generate all of the sites by applying the symmetry operations[5] of D_{2h} to χ,

$$\sigma^{(1)}(E)=\begin{bmatrix}1&0&0\\0&1&0\\0&0&1\end{bmatrix},\quad \sigma^{(2)}(R_y)=\begin{bmatrix}-1&0&0\\0&1&0\\0&0&-1\end{bmatrix},$$
$$\sigma^{(3)}(i)=\begin{bmatrix}-1&0&0\\0&-1&0\\0&0&-1\end{bmatrix},\quad \sigma^{(4)}(iR_y)=\begin{bmatrix}1&0&0\\0&-1&0\\0&0&1\end{bmatrix}, \tag{7}$$

where $\sigma^{(1)}$ is the identity, $\sigma^{(2)}$ is rotation by π about y, $\sigma^{(3)}$ is inversion, and $\sigma^{(4)}$ is $\sigma^{(2)}\times\sigma^{(3)}$ so that sites 3 and 4 are the inversion images of sites 1 and 2, respectively. It is easily shown using (3) that any χ is invariant under inversion since

$$\chi_{ijk}^{(\text{inversion image})}=(-1)(-1)(-1)(-1)\chi_{ijk}=\chi_{ijk} .$$

Thus any two sites related by inversion symmetry will yield the same signal $S=\chi_{ijk}E_iE_jH_k$. This leaves only two sites that are inequivalent. It remains to calculate the polarization of the second site. Using (3), we write

$$\chi_{ijk}^{(2)}=\sigma_{ii}^{(2)}\sigma_{jj}^{(2)}\sigma_{kk}^{(2)}\chi_{ijk}^{(1)}\,|\,\sigma^{(2)}\,|$$

and it follows that

$$P_x^{(2)}=\chi_{xyz}^{(1)}E_yH_z+\chi_{xzy}^{(1)}E_zH_y-\chi_{xxz}^{(1)}E_xH_z ,$$
$$P_y^{(2)}=\chi_{yzx}^{(1)}E_xH_z+\chi_{yzx}^{(1)}E_zH_x-\chi_{yyz}^{(1)}E_yH_z , \tag{8}$$
$$P_z^{(2)}=\chi_{zxy}^{(1)}E_xH_y+\chi_{zyx}^{(1)}E_yH_x-\chi_{zzz}^{(1)}E_zH_z .$$

The total polarization is

$$P^{\text{tot}}=2P^{(1)}+2P^{(2)} .$$

For the experimental conditions[1,2] $\mathbf{E}=(E_x,E_y,0)$ and $\mathbf{H}=(0,0,H_z)$, the signals of the four sites are

$$S^{(1)}=S^{(3)}=(\chi_{xyz}^{(1)}+\chi_{yxz}^{(1)})E_xE_yH_z+\chi_{xxz}^{(1)}E_x^2H_z+\chi_{yyz}^{(1)}E_y^2H_z ,$$
$$S^{(2)}=S^{(4)}=(\chi_{xyz}^{(1)}+\chi_{yxz}^{(1)})E_xE_yH_z-\chi_{xxz}^{(1)}E_x^2H_z-\chi_{yyz}^{(1)}E_y^2H_z . \tag{9}$$

Summing (9) over all four sites, the total signal

$$S=4(\chi_{xyz}^{(1)}+\chi_{yxz}^{(1)})E_xE_yH_z \tag{10}$$

can now be compared to the macroscopic result (5). We thus conclude that

$$(\chi_{xyz}^{(1)}+\chi_{yxz}^{(1)})=\tfrac{1}{4}(\chi_{xyz}+\chi_{yxz})\sim 0$$

and that the remaining contributions of sites 1 and 3 are exactly canceled by sites 2 and 4 so that the macroscopic signal is zero due to site interference. This is also consistent with the observations[1,2] of Pr^{3+}:$YAlO_3$ under a weak static magnetic field. The static field lifts the degeneracy of the two sites and yields signals[1,2] of opposite sign.

In another experimental configuration, $\mathbf{E}=(E_x,E_y,0)$ and $\mathbf{H}=(H_x,H_y,0)$, the theory predicts that $S=\mathbf{P}\cdot\mathbf{E}$ be identically zero for each site. This corresponds to the observation of Zeeman interference[2] in each individual site where positive and negative Zeeman signals exactly cancel in zero static field.

III. Pr^{3+}:LaF_3 AND DETERMINATION OF CRYSTAL SYMMETRY

Consider next the group-theoretical treatment of the Raman heterodyne signal for Pr^{3+}:LaF_3 where again the coordinates (x,y,z) are parallel to the crystal axes (a,b,c). In this case, there is some controversy over the correct assignment of the crystal symmetry. Oftedal[9] and Schlyter[10] report D_{6h}, Mansmann,[11] Zalkin *et al.*,[12] and Reddy and Erickson[13] give D_{3d} from x-ray data, while de Rango *et al.*[14] select C_{6v} from neutron diffraction. The behavior of the Raman heterodyne signal can be used to distinguish between these different possibilities. The symmetries D_{6h} and C_{6v} both belong to the same class of hexagonal symmetry while D_{3d} is a trigonal symmetry (see Table I). The macroscopic signal for arbitrary fields, $\mathbf{E}=(E_x,E_y,E_z)$ and $\mathbf{H}=(H_x,H_y,H_z)$, for D_{6h} and C_{6v} symmetries should obey

$$S=(\chi_{xzy}+\chi_{zxy})(E_xH_y-E_yH_x)E_z , \tag{11}$$

while the signal for the D_{3d} symmetry should obey

$$S=\chi_{xxx}[(E_x^2-E_y^2)H_x-2E_xE_yH_y]+(\chi_{xzy}+\chi_{zxy})(E_xH_y-E_yH_x)E_z . \tag{12}$$

In order to experimentally verify the symmetry, we rewrite these last equations using cylindrical coordinates for the special case $E_z=0$ and $H_z=0$, such that

$$\mathbf{E}=E(\cos\theta,\sin\theta,0),\quad \mathbf{H}=H(\cos\gamma,\sin\gamma,0) .$$

Equations (11) and (12) then become

TABLE I. Raman heterodyne signal $S=\mathbf{P}\cdot\mathbf{E}$ for all crystal symmetries.

1. Triclinic (C_1, S_2)

$$S=(\chi_{xxx}H_x+\chi_{xxy}H_y+\chi_{xxz}H_z)E_x^2+(\chi_{yyx}H_x+\chi_{yyy}H_y+\chi_{yyz}H_z)E_y^2$$
$$+(\chi_{zzx}H_x+\chi_{zzy}H_y+\chi_{zzz}H_z)E_z^2+(\chi_{xyx}+\chi_{yxx})E_xE_yH_x+(\chi_{xyy}+\chi_{yxy})E_xE_yH_y$$
$$+(\chi_{xyz}+\chi_{yxz})E_xE_yH_z+(\chi_{xzx}+\chi_{zxx})E_xE_zH_x+(\chi_{xzy}+\chi_{zxy})E_xE_zH_y$$
$$+(\chi_{xzz}+\chi_{zxz})E_xE_zH_z+(\chi_{yzx}+\chi_{zyx})E_yE_zH_x+(\chi_{yzy}+\chi_{zyy})E_yE_zH_y$$
$$+(\chi_{yzz}+\chi_{zyz})E_yE_zH_z$$

2. Monoclinic (C_2, C_{1h}, C_{2h})

$$S=(\chi_{xxz}E_x^2+\chi_{yyz}E_y^2+\chi_{zzz}E_z^2)H_z+(\chi_{xyz}+\chi_{yxz})E_xE_yH_z+(\chi_{xzx}+\chi_{zxx})E_xE_zH_x$$
$$+(\chi_{yzx}+\chi_{zyx})E_yE_zH_x+(\chi_{xzy}+\chi_{zxy})E_xE_zH_y+(\chi_{yzy}+\chi_{zyy})E_yE_zH_y$$

3. Orthorhombic (D_2, C_{2v}, D_{2h})

$$S=(\chi_{xyz}+\chi_{yxz})E_xE_yH_z+(\chi_{xzy}+\chi_{zxy})E_xE_zH_y+(\chi_{yzx}+\chi_{zyx})E_yE_zH_x$$

4. Tetragonal I (C_4, S_4, C_{4h})

$$S=\chi_{xxz}(E_x^2+E_y^2)H_z+\chi_{zzz}E_z^2H_z+(\chi_{xzx}+\chi_{zxx})(E_xH_x+E_yH_y)E_z$$
$$+(\chi_{xzy}+\chi_{zxy})(E_xH_y-E_yH_x)E_z$$

5. Tetragonal II ($D_4, C_{4v}, D_{2d}, D_{4h}$) and Hexagonal II ($D_6, C_{6v}, D_{3h}, D_{6h}$)

$$S=(\chi_{xzy}+\chi_{zxy})(E_xH_y-E_yH_x)E_z$$

6. Trigonal I (C_3, S_6)

$$S=\chi_{xxx}(E_x^2H_x-2E_xE_yH_y-E_y^2H_x)+\chi_{yyy}(E_y^2H_y-2E_xE_yH_x-E_x^2H_y)$$
$$+\chi_{zzz}E_z^2H_z+\chi_{xxz}(E_x^2+E_y^2)H_z+(\chi_{xzx}+\chi_{zxx})(E_xH_x+E_yH_y)E_z$$
$$+(\chi_{xzy}+\chi_{zxy})(E_xH_y-E_yH_x)E_z$$

7. Trigonal II (D_3, C_{3v}, D_{3d})

$$S=\chi_{xxx}[(E_x^2-E_y^2)H_x-2E_xE_yH_y]+(\chi_{xzy}+\chi_{zxy})(E_xH_y-E_yH_x)E_z$$

8. Hexgonal I (C_6, C_{3h}, C_{6h})

$$S=\chi_{xxz}(E_x^2+E_y^2)H_z+\chi_{zzz}E_z^2H_z$$
$$+[(\chi_{xzx}+\chi_{zxx})(E_xH_x+E_yH_y)+(\chi_{xzy}+\chi_{zxy})(E_xH_y-E_yH_x)]E_z$$

9. Hexgonal II (See No. 5.)

10. Cubic I (T, T_h)

$$S=(\chi_{xyz}+\chi_{xzy})(E_xE_yH_z+E_yE_zH_x+E_xE_zH_y)$$

11. Cubic II (O, T_d, O_h)

$$S=0$$

$$S=0 \quad (D_{6h}, C_{6v}), \tag{13}$$

$$S=\chi_{xxx}E^2H\cos(2\theta+\gamma) \quad (D_{3d}). \tag{14}$$

We see that in a Raman heterodyne experiment with $E_z=0$ and $H_z=0$ the hexagonal symmetries will yield a zero signal while the D_{3d} symmetry will yield a signal that varies sinusoidally in magnitude with rotation of the electric or magnetic field polarization. We have tested the prediction (14) for the ground-state hyperfine $^3H_4\,|\pm\frac{5}{2}\rangle\rightarrow|\pm\frac{3}{2}\rangle$ transitions of Pr^{3+}:LaF_3 by observing a signal whose amplitude displays (Fig. 1) the predicted cosine behavior with period 180° as the laser polarization is rotated. Figure 2 displays how the signal of the other ground-state transition $^3H_4\,|\pm\frac{3}{2}\rangle\rightarrow|\pm\frac{1}{2}\rangle$ changes sign when the polarization is changed by 90°. Since the signal is clearly nonzero, in disagreement with (13), and (14) is verified, the assignment of D_{3d} to the LaF_3 crystal is unambiguous. This case is a clear example of the use of Raman heterodyne interference in elucidating the symmetry properties of crystals.

Based on the choice of host-crystal symmetry,[6] the re-

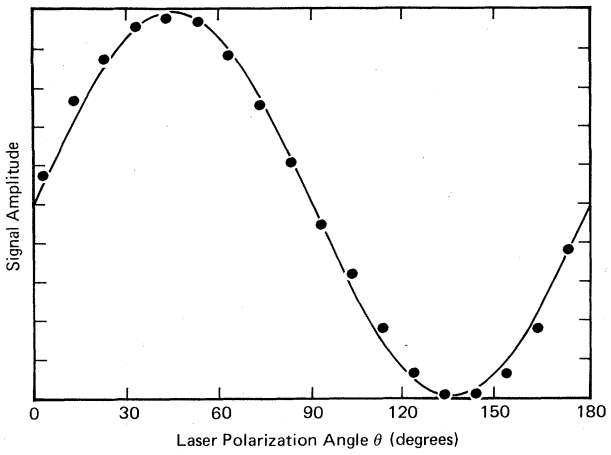

FIG. 1. Maximum amplitude of the Raman heterodyne signal for the $^3H_4 \mid \pm\frac{5}{2}\rangle \rightarrow \mid \pm\frac{3}{2}\rangle$ (16.7 MHz) ground-state transition in Pr^{+3}:LaF_3 as a function of the electric field polarization angle. Circles represent experimental points and the solid line is the best fit of the $\cos(2\theta+\gamma)$ dependence of Eq. (14) to the data. The experimental configuration is $\mathbf{E}=E(\cos\theta,\sin\theta,0)$ with optical power of 10 mW, $\mathbf{H}=H(\cos\gamma,\sin\gamma,0)$, a radiofrequency field $H=0.7$ G, and γ held fixed.

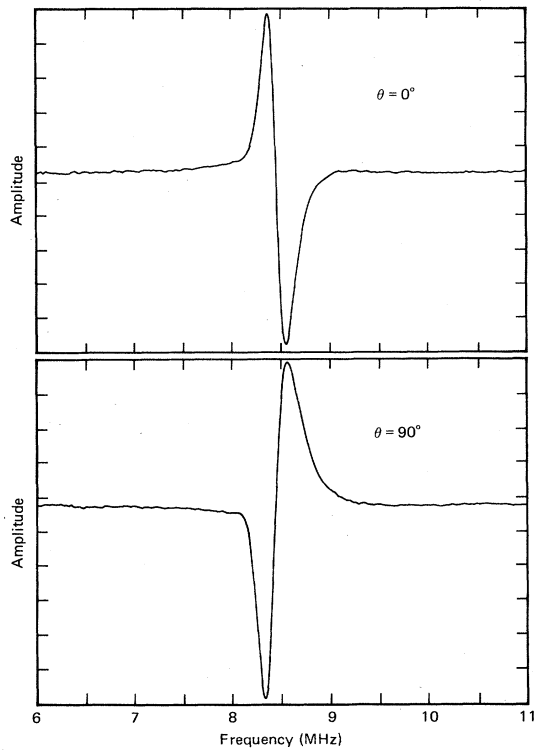

FIG. 2. Line shape of the $^3H_4 \mid \pm\frac{1}{2}\rangle \rightarrow \mid \pm\frac{3}{2}\rangle$ (8.47 MHz) ground-state transition of Pr^{3+}:LaF_3 in dispersive phase showing sign reversal when the electric field polarization is rotated by $\theta=90°$. The experimental configuration is $\mathbf{E}=E(\cos\theta,\sin\theta,0)$ with optical power of 10 mW, $\mathbf{H}=H(\cos\gamma,\sin\gamma,0)$, $H=2.4$ G, and γ held fixed.

sults of nuclear quadrupole resonance work[13] and the observed optical polarization selection rule,[2,15] which we discuss below, the site symmetry in Pr^{3+}:LaF_3 must be C_2. Using this assignment we have calculated the contributions of the sites to the total signal. Here the situation is more complicated. There are six nuclear sites with half of the sites being the inversion image of the other half, leaving a total of three inequivalent sites. For this case the generating matrices for the three inequivalent sites are

$$\sigma^{(1)}(E)=\begin{bmatrix}1&0&0\\0&1&0\\0&0&1\end{bmatrix},$$

$$\sigma^{(2)}(R_3)=\begin{bmatrix}-\frac{1}{2}&\sqrt{3}/2&0\\-\sqrt{3}/2&-\frac{1}{2}&0\\0&0&1\end{bmatrix}, \tag{15}$$

$$\sigma^{(3)}(R_3^2)=\begin{bmatrix}-\frac{1}{2}&-\sqrt{3}/2&0\\\sqrt{3}/2&-\frac{1}{2}&0\\0&0&1\end{bmatrix},$$

where R_3 and R_3^2 represent 120° and 240° rotations about the crystal c axis. We will also make use of an additional restriction for the optical transition $^3H_4(\Gamma_1)\rightarrow{}^1D_2(\Gamma_1)$. Since the initial and final electronic states have Γ_1 symmetry in the C_2 symmetry group, the transition is allowed[13,15] only when $E||C_2$ axis where C_2 of site $1||x$ axis. This restriction has the consequence that for site 1 only the tensor $\chi^{(1)}_{xxx}$ is applicable. Then the signal from site 1 is

$$S^{(1)}=\chi^{(1)}_{xxx}E_x^2H_x\ , \tag{16}$$

while the signals from sites 2 and 3 using (15) and (3) are

$$\begin{aligned}S^{(2)}=\chi^{(1)}_{xxx}[&-\tfrac{1}{8}(E_x^2H_x+3E_y^2H_x+6E_xE_yH_y)\\&-\tfrac{1}{8}\sqrt{3}(E_x^2H_y+3E_y^2H_y+2E_xE_yH_x)]\ ,\\S^{(3)}=\chi^{(1)}_{xxx}[&-\tfrac{1}{8}(E_x^2H_x+3E_y^2H_x+6E_xE_yH_y)\\&+\tfrac{1}{8}\sqrt{3}(E_x^2H_y+3E_y^2H_y+2E_xE_yH_x)]\ .\end{aligned} \tag{17}$$

Using cylindrical coordinates $\mathbf{E}=E(\cos\theta,\sin\theta,0)$ and $\mathbf{H}=H(\cos\gamma,\sin\gamma,0)$, we have

$$\begin{aligned}S^{(2)}&=\chi^{(1)}_{xxx}E^2H\cos^2(\theta+120°)\cos(\gamma+120°)\ ,\\S^{(3)}&=\chi^{(1)}_{xxx}E^2H\cos^2(\theta-120°)\cos(\gamma-120°)\ .\end{aligned} \tag{18}$$

From (18) we see that when $\theta=\gamma=90°$, the electric and magnetic field polarizations are appropriate for these two sites interfering completely. In general, however, the interference is only partial and the signal will be composed of contributions that are not necessarily equal from all three sites.

IV. RAMAN HETERODYNE SIGNAL FOR GENERAL CRYSTAL SYMMETRY

Table I shows the results for the macroscopic signal for any crystal-host symmetry. The 32 point groups are di-

vided into 11 categories according to the symmetry properties of χ. In general, the higher the crystal symmetry, the simpler the expression for the signal and the more likely is the possibility that complete interference can occur for some experimental configuration. In the last group containing the symmetries O, T_d, and O_h, the signal is identically zero regardless of the experimental configuration. For these crystals (examples being CaF_2 and YAG), site interference necessarily occurs when the impurity ion has a site symmetry lower than the host-crystal symmetry, as then the signal of a site does not vanish.

V. CONCLUSIONS

We have shown that interference behavior can be predicted easily using group-theoretical methods. A Raman heterodyne signal can vanish either because of interference when the contributions of the sites exactly cancel or when the signal for each site is zero. When a signal is nonzero, the contributions from the sites are not necessarily equal and partial interference may occur. Furthermore, we have shown that it is easy to determine the behavior of the Raman heterodyne signal as a function of electric and magnetic field polarizations, which can be a useful tool in distinguishing between possible crystal symmetries.

ACKNOWLEDGMENTS

One of us (E.S.K.) acknowledges partial financial support from IBM. This work was supported in part by the U. S. Office of Naval Research.

[1]M. Mitsunaga, E. S. Kintzer, and R. G. Brewer, Phys. Rev. Lett. **52**, 1484 (1984).
[2]M. Mitsunaga, E. S. Kintzer, and R. G. Brewer, preceding paper, Phys. Rev. B **31**, 6947 (1985).
[3]J. Mlynek, N. C. Wong, R. G. DeVoe, E. S. Kintzer, and R. G. Brewer, Phys. Rev. Lett. **50**, 993 (1983); N. C. Wong, E. S. Kintzer, J. Mlynek, R. G. DeVoe, and R. G. Brewer, Phys. Rev. B **28**, 4993 (1983).
[4]D. R. Taylor, Opt. Commun. (to be published).
[5]R. R. Birss, Rep. Prog. Phys. **26**, 307 (1963).
[6]S. Geller and E. A. Wood, Acta Crystallogr. **9**, 563 (1956); R. Diehl and G. Brandt, Mater. Res. Bull. **10**, 85 (1975).
[7]G. H. Dieke, *Spectra and Energy Levels of Rare Earth Ions in Crystals* (Interscience, New York, 1968).
[8]L. E. Erickson, Phys. Rev. B **19**, 4412 (1979).
[9]I. Oftedal, Z. Phys. Chem. Abt. B **13**, 190 (1931).
[10]K. Schlyter, Ark. Kemi **5**, 73 (1952).
[11]M. Mansmann, Z. Kristallogr. **122**, 375 (1965).
[12]A. Zalkin, D. H. Templeton, and T. E. Hopkins, Inorg. Chem. **5**, 1466 (1966).
[13]B. R. Reddy and L. E. Erickson, Phys. Rev. B **27**, 5217 (1983).
[14]C. de Rango, G. Tsoucaris, and Ch. Zelwer, C. R. Acad. Sci. C **263**, 64 (1965).
[15]R. M. Shelby and R. M. Macfarlane, Opt. Commun. **27**, 399 (1978).